

# Interaction-driven Dynamics of $^{40}\text{K} / ^{87}\text{Rb}$ Fermi-Bose Gas Mixtures in the Large Particle Number Limit

C. Ospelkaus, S. Ospelkaus, K. Sengstock and K. Bongs  
*Institut für Laserphysik, Luruper Chaussee 149, 22761 Hamburg / Germany*

We have studied effects of interspecies attraction in a Fermi-Bose mixture over a large regime of particle numbers in the  $^{40}\text{K} / ^{87}\text{Rb}$  system. We report on the observation of a mean field driven collapse at critical particle numbers of  $1.2 \cdot 10^6$   $^{87}\text{Rb}$  atoms in the condensate and  $7.5 \cdot 10^5$   $^{40}\text{K}$  atoms consistent with mean field theory for a scattering length of  $a_{FB} = -281(15) a_0$  [S. Inouye *et al.*, Phys. Rev. Lett. 93, 183201 (2004)]. For large overcritical particle numbers, we see evidence for revivals of the collapse. Part of our detailed study of the decay dynamics and mechanisms is a measurement of the ( $^{87}\text{Rb} - ^{87}\text{Rb} - ^{40}\text{K}$ ) three-body loss coefficient  $K_3 = (2.8 \pm 1.1) \cdot 10^{-28} \text{cm}^6/\text{s}$ , which is an important input parameter for dynamical studies of the system.

PACS numbers: 03.75.Kk, 03.75.Ss, 34.20.Cf, 32.80.Pj

The recent realization of the BCS-BEC-crossover [1] in strongly interacting dilute fermionic gases has allowed intriguing insight into the regime connecting Bose and Fermi superfluidity. Quantum degenerate Fermi-Bose mixtures are expected to offer an alternative and complementary approach to Fermi superfluidity, where the interaction between fermions is mediated by the bosons [2], analogous to the role of phonons in solid state superconductors. The realization of boson-mediated Cooper pairing in optical lattices with tunable interactions through hetero-nuclear Feshbach resonances would open up fascinating perspectives. Furthermore, it has been pointed out that these mixtures exhibit a wealth of novel quantum phases [3].

Exploring these phenomena relies on a detailed understanding of interactions in ultracold Fermi-Bose mixtures which are characterized by two scattering parameters: the s-wave background scattering length for collisions between two bosons  $a_{BB}$  and the Fermi-Bose interspecies scattering length  $a_{FB}$ . For repulsive interspecies interaction, the constituents may phase separate, while an attractive interaction creates an additional mean field confinement and eventually renders the mixture unstable [4, 5], similar to the mean field collapse found in BECs with attractive interaction [6].

The prediction and first experimental confirmation of a large and negative interspecies scattering length [7, 8] shifted the  $^{40}\text{K} / ^{87}\text{Rb}$  system into the focus of scientific interest. In addition to the very precisely known  $a_{BB} = 98.98(04) a_0$  [9], the value of  $a_{FB}$  is of paramount importance for this system, setting maximum achievable particle numbers but also determining correlations and excitations. Published critical particle numbers for the occurrence of a mean field collapse ( $N_K \approx 2 \cdot 10^4$  and  $N_{Rb} \approx 10^5$  [10]) appeared to impose severe constraints on maximally achievable particle numbers, but at the same time seemed to indicate an excitingly large value of  $a_{FB} = -395(15) a_0$  [11]. There is however an ongoing controversy in the scientific community caused by recent reports on the observation of stable mixtures at

higher particle numbers [11, 12] and measurements of  $a_{FB} = -250(30) a_0$  [12] using thermal relaxation and  $a_{FB} = -281(15) a_0$  [13] using Feshbach spectroscopy methods. A detailed exploration of the regime of mean field instability is not only interesting in itself due to its strong dependence on the interaction parameters and due to the dynamical behavior when the instability occurs. More generally, it is a fundamental prerequisite for a full understanding of  $^{40}\text{K} / ^{87}\text{Rb}$ -mixtures and the controlled achievement of fascinating physics in the regime of large particle numbers and strong interactions, e.g. the realization of mixed bright solitons [14] and the observation of Fermi-Bose correlations up to novel BCS phases in optical lattices.

In this letter, we report on reaching the to our knowledge so far highest particle numbers in the  $^{40}\text{K} / ^{87}\text{Rb}$  system only limited by the onset of instability, which we find consistent with  $a_{FB} \approx -281 a_0$  [13]. Right at the phase transition point of a large bosonic thermal cloud ( $n \approx 4 \cdot 10^{14} \text{cm}^{-3}$ ), we observe a strong dynamical modification of the in-trap fermionic distribution due to the mean-field interaction with the bosons. At even higher densities, we observe enhanced localized loss processes in the overlap region of the BEC and the Fermi gas, which we ascribe to a mean field collapse based on lifetime and dynamical arguments as well as comparison to theory. After the collapse, we observe a peaked density distribution of the Fermi cloud subjected to the strong localized mean field potential of the condensate. In addition, we present a novel measurement of the three-body inelastic K-Rb decay constant differing by an order of magnitude from the value given in [10].

Our setup is based on a two-species 2D/3D-MOT geometry [15], where the  $^{40}\text{K}$  vapor is produced using self-made enriched  $^{40}\text{K}$  dispensers [16]. In the 3D-MOT, we achieve  $1 \cdot 10^{10}$   $^{87}\text{Rb}$  and  $2 \cdot 10^8$  fermionic  $^{40}\text{K}$  atoms within 10 seconds. The pre-cooled mixture is loaded into a Ioffe-Pritchard type magnetic trap (cloverleaf / 4D-hybrid,  $\nu_{\text{ax}}^{\text{Rb}} = 11.3 \text{Hz}$  and  $\nu_{\text{rad}}^{\text{Rb}} = 257 \text{Hz}$ , i.e.  $\nu_{\text{ax}}^{\text{K}} = 16.6 \text{Hz}$  and  $\nu_{\text{ax}}^{\text{K}} = 378 \text{Hz}$ ) for RF-induced sympathetic cooling

of  $^{40}\text{K}$  in the  $|F = 9/2, m_F = 9/2\rangle$  state with  $^{87}\text{Rb}$  in the  $|F = 2, m_F = 2\rangle$  state. If all of the  $^{87}\text{Rb}$  atoms are removed, we currently obtain Fermi gases of up to  $3 \cdot 10^6$   $^{40}\text{K}$  atoms at  $T/T_F = 0.2$  or  $9 \cdot 10^5$  at  $T/T_F = 0.1$ .

When the  $^{87}\text{Rb}$  atoms are not completely evaporated, various regimes of mixtures are accessible, ranging from dense thermal  $^{87}\text{Rb}$  clouds of  $10^7$   $^{87}\text{Rb}$  atoms right at the phase transition point interacting with a moderately degenerate Fermi gas of  $2 \cdot 10^6$   $^{40}\text{K}$  atoms to deeply degenerate mixtures with almost pure condensates. We achieve  $> 1 \cdot 10^6$  atoms in the condensate coexisting with  $7.5 \cdot 10^5$   $^{40}\text{K}$  atoms, limited by the onset of the collapse.

In a first set of experiments, shown in Fig. 1, we analyze the behavior of the mixture in these regimes during the evaporation ramp, similar to the procedure in [10]. In our case the dynamics becomes clearly visible in the axial  $^{40}\text{K}$  density distribution, which due to the relatively short time of flight (TOF) should closely reflect the in trap distribution. The fast ramp speed (1 MHz/s) in this experiment means that we are potentially dealing with strongly out of equilibrium samples. Already at the phase transition point (a) of the bosonic cloud, we observe strong distortions of the axial  $^{40}\text{K}$  density profile. The profile looks like a chopped off Fermi profile with a peak in the center of the flat top which we ascribe to the interaction with the bosonic component (peak density  $\approx 4 \cdot 10^{14} \text{ cm}^{-3}$ ). For a large BEC (b) the  $^{40}\text{K}$  profile exhibits a pronounced hole in the trap center which we ascribe to a strong localized loss process due to the interaction with the BEC. These losses are too fast for transport in the slow axial direction to be able to continuously maintain the undisturbed density profile by refilling the center of the trap from the outer regions. As we shall see, this fast loss (e. g. from Fig. 2  $\leq 10$  ms) is a signature of the mean field collapse of the mixture. After the collapse, we observe that  $^{40}\text{K}$  distributions sharply peaked in the center remain stable for relatively long timescales exceeding 100 ms (c). A Fermi-Dirac fit to the data is shown as a dotted line for comparison. We attribute this peaked distribution to the Fermi-Bose attraction creating an additional trapping potential for the fermions (“mean field dimple” in the magnetic trap potential).

The strong depletion of the Fermi cloud in the center is accompanied by rapid particle loss of approximately two thirds of the fermionic particle number. We ascribe this loss to the mean field collapse of the mixture. Beyond critical particle numbers, the mean field potential is no longer balanced by the repulsive interaction in the  $^{87}\text{Rb}$  BEC and the outward bound Fermi pressure, so that the part of the mixture overlapping with the BEC contracts rapidly to such large densities that enormous 3-body losses reduce the overall particle number in this region to an undercritical value. It is therefore natural that we observe the collapse in the vicinity of strong contracting mean field effects of the Bose gas on the fermionic distribution (see Fig. 1a, c; cf. [17]). Although the en-

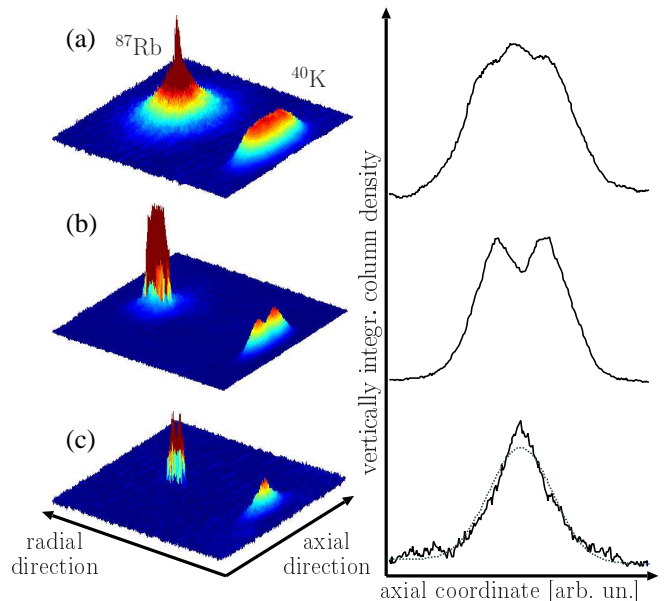


FIG. 1: Typical evolution of an overcritical mixture after an evaporation ramp (rate -1 MHz/s) stopped and held fixed for 15 ms at 80 kHz (a), 50 kHz (b) and 20 kHz (c) above the  $^{87}\text{Rb}$  trap bottom of 490 kHz. Left-hand side: 3D representation of absorption images with false-color coding of the optical density.  $^{87}\text{Rb}$  and  $^{40}\text{K}$  images are taken in the same run, although at different TOF: 20ms ( $^{87}\text{Rb}$ ) and 3 – 5ms ( $^{40}\text{K}$ ). Right-hand side: corresponding axial line profiles integrated along the vertical direction.

semble is out of equilibrium and shows very complex dynamics *after* this rapid loss [18], one can intuitively imagine that the Fermi distribution depleted in the center of the cloud is refilled from the outside parts of the sample on a timescale related to the axial trap frequency, possibly leading to repeated local collapses, until the mixture will become undercritical and reestablish an equilibrium situation. In order to observe this phenomenon we have prepared a mixture where the bosonic part ( $\approx 10^7$  atoms) has only started condensing and observed the evolution of the ensemble at constant evaporation frequency. As the condensate grows due to the mild remaining evaporative cooling, it reaches the critical particle number of  $N_B = 1.2 \cdot 10^6$ . Due to the near-equilibrium situation before, the collapse now only leads to a relatively small loss in total particle number but is still clearly visible in the  $^{40}\text{K}$  atom number integrated over the central part of the TOF image as shown in Fig. 2. After the first collapse this number remains constant for some time and then drops abruptly again [26]. Such “revivals” of the collapse have been predicted in a recent numerical analysis of the collapse dynamics ([18], see inset in Fig. 2), although in a spherically symmetric configuration with  $\nu_{\text{Rb}} = 100$  Hz.

Analysis of similar decay series in various particle num-

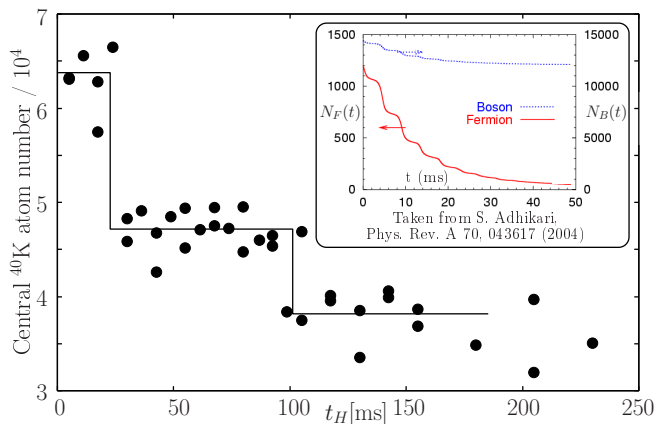


FIG. 2: Decay of the fermionic component in a slightly over-critical mixture. The first sudden drop is the initial collapse; the second drop is one “revival” of the collapse. The line is to guide the eye. For comparison, the inset shows results from dynamical modelling of the collapse.

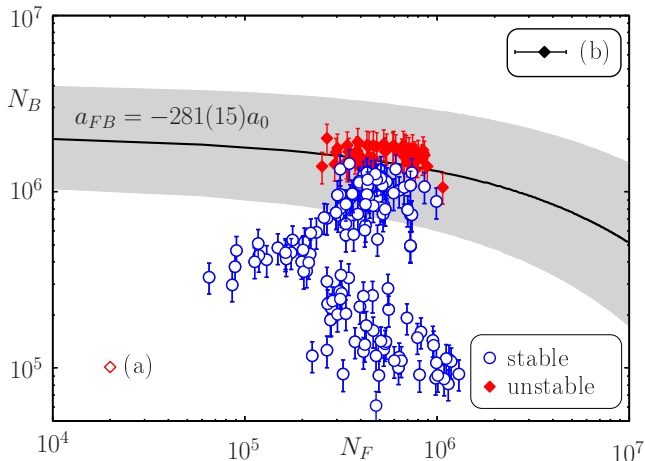


FIG. 3: Stability diagram for the  $^{40}\text{K} / ^{87}\text{Rb}$  mixture. The uncertainty in  $N_{\text{Rb}}/N_{\text{K}}$  is assumed to be 20%/30%. The error on  $N_{\text{F}}$  is not critical and is given exemplarily in (b). The solid black line is based on the theory of ref. [19] and  $a_{\text{FB}} = -281(15)a_0$  [13]. (a) is the critical particle number reported in ref. [10] (here the trap had a different aspect ratio, but a similar mean trapping frequency  $\bar{\nu}_{\text{K}} = 134$  Hz, as compared to our experiment with  $\bar{\nu}_{\text{K}} = 133$  Hz)

ber regimes enables us to extract a value for the critical particle numbers for the onset of the collapse. Our findings are summarized in Fig. 3. Situations where the decay is compatible with 3-body decay of an undisturbed density distribution are identified as stable. If the loss is incompatible with 3-body decay, the situations are identified as unstable. Note that the time scales for the two situations are clearly different, varying from a few 100 ms for the stable cases to about 20 ms for the

unstable cases. The solid line in Fig. 3 is the theoretical stability limit for our trapping conditions, based on [19] and the following approximation to the fermionic chemical potential:  $\mu_{\text{F}} = \mu_{\text{F},0} - (g_{\text{FB}}/g_{\text{BB}}) \cdot \mu_{\text{B},0}$  where  $\mu_{\text{F},0}$  and  $\mu_{\text{B},0}$  are the Fermion / Boson non-interacting chemical potentials and  $g_{\text{FB}}$  and  $g_{\text{BB}}$  are the standard coupling constants [20, 21]. The curve is plotted for the value  $a_{\text{FB}} = -281 a_0$ ; a confidence interval for the stability border based on the uncertainty of  $15a_0$  on  $a_{\text{FB}}$  [13] is indicated in grey. Our findings for the critical particle numbers are clearly consistent with mean-field theory of the collapse based on this value for  $a_{\text{FB}}$  [27].

Three-body decay is the underlying loss mechanism for the collapse of the mixture. The value of the associated rate coefficient is therefore an important input parameter for detailed understanding of the dynamical behavior of the collapse (“revivals”) [18]. In order to minimize experimental uncertainties, we extract the value for the 3-body rate coefficient from the decay of *non-degenerate thermal ensembles* in an equilibrium situation over a large range of densities. Since collisions involving two identical fermions are strongly suppressed due to the Pauli exclusion principle [23, 24], we consider only inelastic collisions between two bosons and one fermion. For pure 3-body loss, the decay process is then characterized by the following rate equation:

$$\frac{\dot{N}_{\text{F}}(t)}{N_{\text{F}}(t)} = -\tau^{-1} - K_3 \cdot \int d^3r n_{\text{B}}^2(r, t) \frac{n_{\text{F}}(r, t)}{N_{\text{F}}(t)}$$

where  $n_{\text{B}}$  and  $n_{\text{F}}$  are the respective densities,  $K_3$  is the rate coefficient for three-body loss and  $\tau$  the background collisional lifetime. Integrating this equation over time yields

$$\ln \frac{N_{\text{F}}(t)}{N_{\text{F}}(0)} + \frac{t}{\tau} = -K_3 \cdot \int_0^t dt' \int d^3r n_{\text{B}}^2(r, t') \cdot \frac{n_{\text{F}}(r, t')}{N_{\text{F}}(t')}$$

Based on the measured background scattering rate, the left-hand side expression can be evaluated at any given time  $T$  for a decay series. The right-hand side inner integral is evaluated using an equilibrium Fermi-Dirac profile for  $^{40}\text{K}$  and a Bose-enhanced thermal profile for  $^{87}\text{Rb}$  at different time values  $t_i$ . The density distributions are based on the measured temperatures and total atom numbers at  $t_i$ . The outer integral is evaluated by using a piecewise linear interpolation between the discrete values of the inner integral. Plotting the right-hand side as a function of the double integral, we obtain  $K_3$  as the slope of the linear plot (see inset (a) in figure 4). Note that our measurement does not depend on the potassium atom number calibration. As far as the  $^{87}\text{Rb}$  atom number calibration is concerned, we reproduce the measurement of  $^{87}\text{Rb}$  3-body decay from ref. [22]. We find a value of  $K_3 = (2.8 \pm 1.1) \cdot 10^{-28} \text{ cm}^6/\text{s}$  [28], nearly an order of magnitude lower than the value found in [10].

The additional analysis of decay in degenerate samples at higher densities reproduces this result as long as the

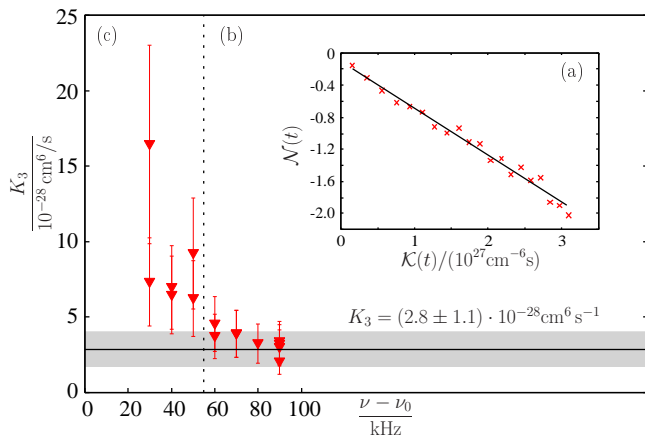


FIG. 4: Extraction of 3-body inelastic loss rate. (a) decay analysis of a thermal sample, where  $\mathcal{N}(t) = \ln \frac{N_F(t)}{N_F(0)} + \frac{t}{\tau}$  and  $\mathcal{K}(t) = N_F^{-1} \cdot \int_0^t dt' \int d^3 r n_b^2(r, t') \cdot n_F(r, t')$  (b)  $K_3$  values extracted in the moderately degenerate and stable regime with peak BEC densities of up to  $4 \cdot 10^{14} \text{cm}^{-3}$  are compatible with the thermal  $K_3$  average (solid line). (c) For low evaporation end frequencies and BEC densities of  $\approx 5 - 7 \cdot 10^{14} \text{cm}^{-3}$ , samples are unstable with respect to the collapse.

mixture is stable (4b), but shows significant deviations for unstable mixtures (4c). In the regime of instability, our analysis of the loss process is no longer valid. Due to the strongly depleted  $^{40}\text{K}$  density distribution, our analysis, relying on undisturbed density distributions, overestimates the density overlap integrals which should lead to a too low value of  $K_3$  as extracted from the decay. Instead, as can be seen from Fig. 4c,  $K_3$  increases below evaporation end frequencies of 60 kHz (high initial densities), proving that the underlying very fast loss mechanism is due to the collapse.

In conclusion, we have presented measurements covering the so far highest particle numbers available in quantum degenerate  $^{40}\text{K}$ - $^{87}\text{Rb}$  Fermi-Bose mixtures leading from stability to collapse. Our measurements of critical particle numbers are consistent with a mean field model of the collapse based on the value of the scattering length  $a_{FB} = -281(15) a_0$  obtained from Feshbach resonance data [13]. This settles the clear discrepancy between the theoretical description of the collapse based on the above interspecies scattering parameter and the critical particle numbers for the mean field collapse reported in an earlier experiment [10] (see Fig. 3a) and indicates that these findings might be influenced by some additional interesting effect. Part of our detailed study of the mixture is a quantitative analysis of three-body loss leading to an order of magnitude lower value than in [10]. Our findings indicate that a wide range of filling factors in large-volume optical lattices ranging in principle up to 2 are possible for the  $^{40}\text{K}$ - $^{87}\text{Rb}$  system. Progress towards loading the mixture into a 3D optical lattice is currently

under way in several labs. Finally, reaching the regime of mean field collapse also lays the ground for the realization of bright solitonlike structures in a quasi 1D geometry [14].

We thank K. Hofmann and B. Albert for help with enriched dispenser production. We acknowledge discussions with M. Brewczyk, M. Gajda, K. Rzażewski and J. M. Goldwin as well as contributions by R. Dinter, P. Ernst, J. Fuchs, M. Nakat, M. Succo, O. Wille and funding by DFG under SPP 1116.

- [1] C. A. Regal *et al.*, Phys. Rev. Lett. **92**, 040403 (2004); M. W. Zwierlein *et al.*, Phys. Rev. Lett. **92**, 120403 (2004); C. Chin *et al.*, Science **305**, 1128 (2004); T. Bourdel *et al.*, Phys. Rev. Lett. **93**, 050401 (2004); J. Kinast *et al.*, Science **307**, 1296 (2005).
- [2] L. Viverit, Phys. Rev. A **66**, 023605 (2002); M. J. Bijlsma *et al.*, Phys. Rev. A **61**, 053601 (2000); D. V. Efremov and L. Viverit, Phys. Rev. B **65**, 134519 (2002).
- [3] A. Albus *et al.*, Phys. Rev. A **68**, 023606 (2003); R. Roth, and K. Burnett, Phys. Rev. A **69**, 021601(R) (2004); F. Illuminati, and A. Albus, Phys. Rev. Lett. **93**, 090406 (2004); M. Lewenstein *et al.*, Phys. Rev. Lett. **92**, 050401 (2004); D. B. M. Dickerscheid *et al.*, Phys. Rev. Lett. **94**, 230404 (2005).
- [4] K. Mølmer, Phys. Rev. Lett. **80**, 1804 (1998).
- [5] R. Roth, Phys. Rev. A **66**, 013614 (2002).
- [6] C. A. Sackett *et al.*, Phys. Rev. Lett. **82**, 876 (1999); E. A. Donley *et al.*, Nature **412**, 295 (2001).
- [7] G. Ferrari *et al.*, Phys. Rev. Lett. **89**, 053202 (2002).
- [8] T. Karpiuk, F. Riboli, G. Modugno, and M. Inguscio, Phys. Rev. Lett. **89**, 150403 (2002).
- [9] E. G. M. van Kempen *et al.*, Phys. Rev. Lett. **88**, 093201 (2002).
- [10] G. Modugno *et al.*, Science **297**, 2240 (2002).
- [11] M. Modugno *et al.*, Phys. Rev. A **68**, 043626 (2003).
- [12] J. Goldwin *et al.*, Phys. Rev. A **70**, 021601 (2004).
- [13] S. Inouye *et al.*, Phys. Rev. Lett. **93**, 183201 (2004).
- [14] T. Karpiuk *et al.*, Phys. Rev. Lett. **93**, 100401 (2004).
- [15] K. Dieckmann *et al.*, Phys. Rev. A **58**, p. 3891 (1998).
- [16] B. DeMarco *et al.*, Rev. Sci. Instr. **70**, 1967 (1999).
- [17] F. Ferlaino *et al.*, Phys. Rev. Lett. **92**, 140405 (2004).
- [18] S. K. Adhikari, Phys. Rev. A **70**, 043617 (2004).
- [19] S. T. Chui, V. N. Ryzhov, and E. E. Tareyeva, JETP Lett. **80**, 274 (2004).
- [20] J. M. Goldwin, Ph.D. thesis, Faculty of the Graduate School of the University of Colorado (2005).
- [21] F. Matera, Phys. Rev. A **68**, 043624 (2003).
- [22] J. Söding *et al.*, Appl. Phys. B **69**, 257 (1999).
- [23] D. Petrov, Phys. Rev. A **67**, 010703(R) (2003).
- [24] J. P. D’Incao and B. D. Esry, cond-mat/0508474 (2005).
- [25] T. Karpiuk *et al.*, J. Phys. B **38**, L215 (2005).
- [26] The refilling is not visible for the chosen integration area.
- [27] Using [19], our critical particle numbers yield  $a_{FB} = -284 a_0$ ; using [25], we obtain  $a_{FB} = -294 a_0$ .
- [28] A 2-body decay analysis leads to a large density-dependent variation (by a factor of 40) of the  $K_2$ -values, indicating that the decay is predominantly 3-body.